

BL LAC CANDIDATES FOR TEV OBSERVATIONS

F. MASSARO¹, A. PAGGI², M. ERRANDO³, R. D'ABRUSCO², N. MASETTI⁴, G. TOSTI^{5,6}, & S. FUNK¹

version September 4, 2018 : fm

ABSTRACT

BL Lac objects are the most numerous class of extragalactic TeV-detected sources. One of the biggest difficulties in investigating their TeV emission resides in their limited number, since only 47 BL Lacs are known as TeV emitters. In this paper, we propose new criteria to select TeV BL Lac candidates based on the infrared (IR) and X-ray observations. We apply our selection criteria to the BL Lac objects listed in the ROMA-BZCAT catalog so identifying 41 potential TeV emitters. We then consider a search over a more extended sample combining the ROSAT bright source catalog and the *WISE* all-sky survey revealing 54 additional candidates for TeV observations. Our investigation also led to a tentative classification of 16 unidentified X-ray sources as BL Lac candidates. This analysis provides new interesting BL Lac targets for future observations with ground based Cherenkov telescopes.

Subject headings: galaxies: active - galaxies: BL Lacertae objects - X-rays: galaxies: individual: - radiation mechanisms: non-thermal

1. INTRODUCTION

BL Lac objects are characterized by very peculiar properties with respect to other classes of active galactic nuclei (AGNs). They are compact, core dominated radio sources, many of them exhibiting superluminal motion and showing rapid and large-amplitude flux variability from radio up to TeV energies, and significant radio to optical polarization (e.g., Blandford & Rees 1978; Urry & Padovani 1995). Their spectral energy distribution (SED) exhibits two main components: the low energy one peaking in the infrared-X-ray energy range, and the second one dominated by γ -rays. Their optical spectra appear to be featureless or with very weak absorption lines (Stoke et al. 1991; Stickel et al. 1991; Laurent-Muehleisen et al. 1999).

According to Padovani & Giommi (1995) BL Lacs can be classified as “Low-frequency peaked BL Lacs” (LBLs) and “High-frequency peaked BL Lacs” (HBLs), depending on whether their broadband radio-to-X-ray spectral index is larger than or smaller than 0.75, respectively.

At very high energies (i.e., $E > 100$ GeV) BL Lac objects, and in particular, HBLs, constitute the largest known population of TeV extragalactic sources, detected by ground based Cherenkov telescopes as HESS, MAGIC and VERITAS. In the following, we refer to the HBLs detected at TeV energies as TBLs while we indicate the HBL candidates for TeV observations as TBCs.

Recently, using the *WISE* point source catalog, which mapped the sky in four different bands centered at 3.4, 4.6, 12, and 22 μm (Wright et al. 2010;

Cutri et al. 2012), we discovered that γ -ray emitting blazars occupy a distinct region in the two-dimensional color-color diagrams, which is well separated from other extragalactic sources whose IR emission is dominated by thermal radiation (“the *WISE* Gamma-ray Strip”, Massaro et al. 2011a; D’Abrusco et al. 2012) and we have developed a method for identifying γ -ray blazar candidates by studying the *WISE* three-dimensional IR color space using the *WISE* Fermi Blazar Sample (i.e., “locus”, see D’Abrusco et al. 2013). This discovery constitutes the basis of our selection criterion for the TBCs.

In this paper, we combine IR and X-ray archival data available in literature to build a criterion useful to find new TBCs. We use the X-ray observations performed with ROSAT along with those from the Wide Infrared Survey Explorer (*WISE*) satellite (Wright et al. 2010).

This paper is organized as follows: in § 2 we investigate the IR properties of the BL Lacs already detected at TeV energies introducing the “ Φ_{XIR} parameter” to distinguish between LBLs and HBLs. In § 3 we outline our criterion to identify TBCs and apply it to the BL Lacs listed in the ROMA-BZCAT⁶ (e.g., Massaro et al. 2011b) and comparisons with selection criteria previously published are presented in § 4. § 5 is dedicated to the all-sky search of new TBL candidates using the combination of the ROSAT bright source catalog (Voges et al. 1999) and the *WISE* all-sky survey (Wright et al. 2010) and § 6 is devoted to our summary and conclusions.

WISE magnitudes are in the Vega system and we use cgs units for our numerical results unless stated otherwise. We assume a flat cosmology with $H_0 = 72$ km s^{-1} Mpc^{-1} , $\Omega_M = 0.26$ and $\Omega_\Lambda = 0.74$ (Dunkley et al. 2009). Spectral indices, α , are defined by flux density, $S_\nu \propto \nu^{-\alpha}$. Frequent acronyms are listed in Table 1.

2. TEV BL LAC OBJECTS

According to the online catalog of TeV-emitting

⁶ <http://www.asdc.asi.it/bzcat/>

¹ SLAC National Laboratory and Kavli Institute for Particle Astrophysics and Cosmology, 2575 Sand Hill Road, Menlo Park, CA 94025, USA

² Smithsonian Astrophysical Observatory, 60 Garden Street, Cambridge, MA 02138, USA

³ Department of Physics and Astronomy, Barnard College, Columbia University, New York, NY 10027, USA

⁴ INAF - Istituto di Astrofisica Spaziale e Fisica Cosmica di Bologna, via Gobetti 101, 40129, Bologna, Italy

⁵ Dipartimento di Fisica, Università degli Studi di Perugia, 06123 Perugia, Italy

TABLE 1
LIST OF ACRONYMS.

Name	Acronym
High Frequency Peaked BL Lac	HBL
Low Frequency Peaked BL Lac	LBL
HBL detected at TeV energies	TBL
HBL candidate for TeV observations	TBC

γ -ray sources (TeVCat)⁷, the number of sources classified as BL Lac objects in the ROMA-BZCAT (Massaro et al. 2009; Massaro et al. 2010; Massaro et al. 2011b) and detected at TeV energies is 42, as of December 2012; these TeV BL Lac objects are listed in Table 2 together with their salient parameters. They have a unique *WISE* counterpart detected at least at 3.4, 4.6 and 12 μm within a radius of $3''.3$ from the ROMA-BZCAT positions (see D’Abrusco et al. 2013, for more details about the ROMA-BZCAT - *WISE* positional associations). They also have a radio counterpart and are detected in the X-ray band by ROSAT (Voges et al. 1999) as reported in the ROMA-BZCAT (Massaro et al. 2011b) with the only exception of MAGICJ2001+435. Thirty-seven of them are also detected in γ rays between 30 MeV and 100 GeV as reported in the *Fermi*-LAT second source Catalog (2FGL; Nolan et al. 2012) and in the second *Fermi*-LAT AGN catalog (2LAC; Ackermann et al. 2011).

2.1. X-ray-to-infrared flux ratio: Φ_{XIR}

Maselli et al. (2010a) defined the ratio Φ_{XR} between the ROSAT X-ray flux F_X and the radio flux density $S_{1.4}$ (at 1.4 GHz), computed using the values reported in the ROMA-BZCAT, to distinguish between HBLs (i.e., $\Phi_{XR} \geq 0.1$) and LBLs (i.e., $\Phi_{XR} < 0.1$). However, this distinction cannot be easily extended all-sky because it does need radio observations at 1.4 GHz which are not always available. To avoid this problem we define a new parameter to distinguish between the two subclasses of BL Lac objects based on the IR observations of *WISE*. It is worth noting that among the BL Lac objects the HBLs are the most detected at TeV energies.

For all the TeV BL Lac objects listed in Table 2, we computed Φ_{XIR} , defined as the ratio between the ROSAT X-ray flux F_X (0.1 - 2.4 keV) and the integrated IR flux F_{IR} between 3.4 and 12 μm , both in units of $10^{-12} \text{ erg cm}^{-2} \text{ s}^{-1}$. This parameter is used to distinguish between HBLs and LBLs instead of Φ_{XR} . We note that sources with $\Phi_{XIR} > 0.1$ in Table 2 have a $\Phi_{XR} > 0.08$ in agreement with the previous classification (Maselli et al. 2010a; Maselli et al. 2010b). We then consider a new classification, labeling as HBLs those having $\Phi_{XIR} > 0.1$ while indicating as LBLs those with $\Phi_{XIR} < 0.1$. An additional justification on the choice of Φ_{XIR} to classify BL Lacs is given in Appendix on the basis of their spectral shape.

2.2. TBL sample selection

We define a clean sample of 33 HBLs TeV detected (i.e., TBLs) out of 42 TeV sources including only:

- having $\Phi_{XIR} > 0.1$;

⁷ <http://tevcats.uchicago.edu/>

- with *WISE* magnitudes lower than 13.32 mag, 12.64 mag and 10.76 mag at 3.4 μm , 4.6 μm and 12 μm , respectively;
- with IR colors between $0.22 \text{ mag} < [3.4]-[4.6] < 0.86 \text{ mag}$, $1.60 \text{ mag} < [4.6]-[12] < 2.32 \text{ mag}$.

The above criterion of TBLs, not only based on the Φ_{XR} ratio, permits to select bright IR sources having the first SED peak between the UV and the X-rays. The minimum X-ray and IR fluxes of the resulting sample are $2.45 \cdot 10^{-12} \text{ erg cm}^{-2} \text{ s}^{-1}$ and $9.47 \cdot 10^{-13} \text{ erg cm}^{-2} \text{ s}^{-1}$, respectively.

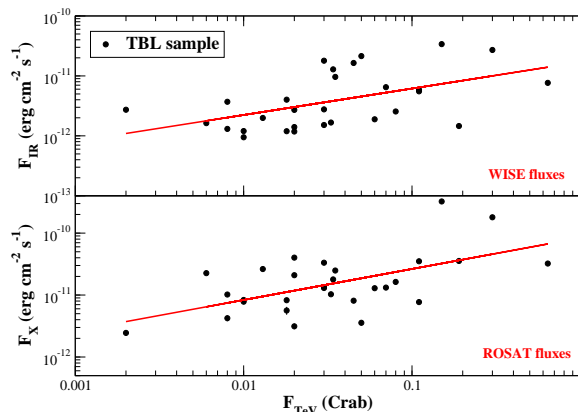


FIG. 1.— The correlations between the IR (upper panel) and the X-ray (lower panel) fluxes with the TeV flux, reported in the *WISE* ROSAT and TeVCat catalogs, respectively (see also Table 2). Regression lines are shown in red (see Section 2.2 for more details).

As shown in Figure 1, there is a hint of a correlation between the IR and TeV fluxes for the TBLs whose measurements were available in TeVCat (see also Table 2), with a correlation coefficient of 0.51. This suggests a good match between *WISE* and the TeV observations. As expected there is also a trend between the ROSAT and the TeV fluxes, with a correlation coefficient of 0.58.

2.3. Infrared colors of TBLs

Recently, we discovered that the γ -ray BL Lac objects lie in a region (i.e., the *WISE* Gamma-ray Strip) of the $[3.4]-[4.6]-[12] \mu\text{m}$ color-color diagram well differentiated from that occupied by generic IR sources (Massaro et al. 2011a). In particular, TBLs are more concentrated near the tail of the *WISE* Gamma-ray Strip. In Figure 2 we show the IR colors of TBLs and those of γ -ray BL Lacs detected by *Fermi* in the 2LAC CLEAN sample that belong to the *WISE* Gamma-ray Strip (D’Abrusco et al. 2013).

We calculated a linear regression in the $[3.4]-[4.6]-[12] \mu\text{m}$ color-color plot for the 33 selected TBLs as shown in Figure 2. We then define the δ parameter according to the equation:

$$\delta = |D \cdot D_{max}^{-1}| \quad (1)$$

where D is the distance between the IR colors of each source in the $[3.4]-[4.6]-[12] \mu\text{m}$ color-color diagram and

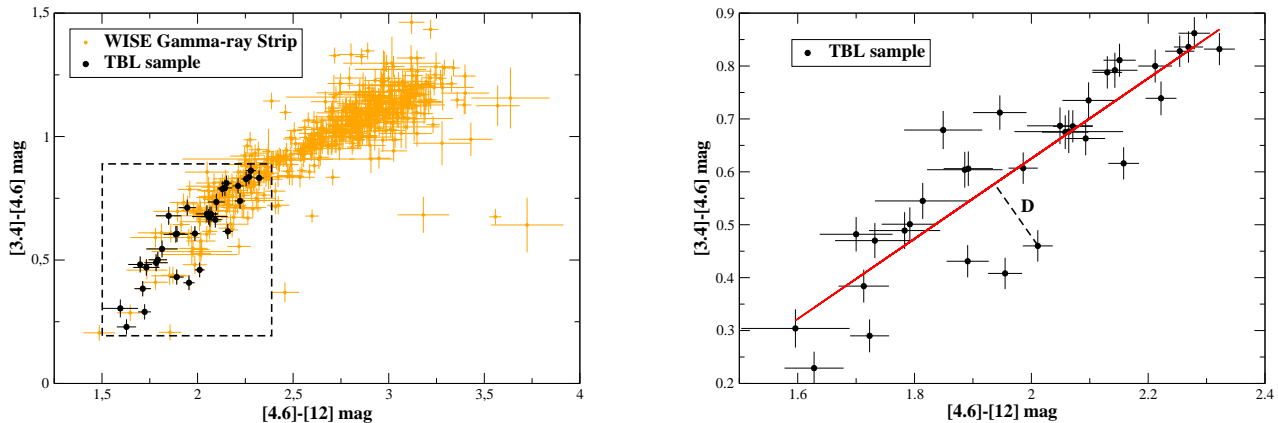


FIG. 2.— Left panel: the $[3.4]-[4.6]-[12]$ μm color-color plot for the 33 TBLs selected (black circles) overlaid to the γ -ray emitting blazars associated with *WISE* source that constitute the *WISE* Gamma-ray Strip (see Massaro et al. 2011a; D’Abrusco et al. 2012; D’Abrusco et al. 2013, for more details). The black dashed box indicates the subregion of the *WISE* Gamma-ray Strip considered in our TBC selection. Right panel: the $[3.4]-[4.6]-[12]$ μm color-color plot for the 33 TBLs selected (black circles). The red line corresponds to the regression line evaluated while the dashed line indicates the distance D between a source and the regression line as described in § 2.3.

the regression line, and D_{max} is the maximum value evaluated only for the selected TBLs (i.e., 0.116 mag). All the TBLs have therefore a value of $\delta < 1.0$ by definition. We verified the residuals of the points in the $[3.4]-[4.6]-[12]$ μm color-color plot with respect to the regression line using a *runs test* and we found that they are randomly distributed at 97% level of confidence⁸.

Finally, we note that $\delta=0.28$ corresponds to the 68% level of confidence (i.e., 1σ) with respect to the regression line and consequently the choice of $\delta=1$ implies that all the TBLs lie within 3.5σ .

3. TBL CANDIDATES SELECTED FROM THE ROMA-BZCAT CATALOG

On the basis of the combined IR and X-ray properties of TBLs (see § 2), we outline the following criteria to select TBL candidates (TBCs). Our selection of TBCs includes all sources that fulfill all following criteria:

1. classified as BL Lac (i.e., BZB) according to the ROMA-BZCAT catalog;
2. have a *WISE* counterpart within $3.3''$ from the ROMA-BZCAT position, detected with Vega magnitudes smaller than 13.318, 12.642 and 10.760 at $3.4\mu\text{m}$, $4.6\mu\text{m}$ and $12\mu\text{m}$, respectively;
3. have IR colors similar to those of TBLs defined by: $0.22 \text{ mag} < [3.4]-[4.6] < 0.86 \text{ mag}$, $1.60 \text{ mag} < [4.6]-[12] < 2.32 \text{ mag}$, respectively;
4. have values of the parameter $\delta < 1$, according to the definition proposed in § 2.3;
5. have X-ray fluxes larger than the minimum value observed for TBLs (i.e., $2.45 \cdot 10^{-12} \text{ erg cm}^{-2} \text{ s}^{-1}$).

⁸ The *runs test* is a non-parametric statistical test that verifies the hypothesis that the elements of the sequence are mutually independent and it could be applied in combination with a regression analysis to check that residuals are randomly distributed as expected in a Gaussian statistic.

The requirement on the X-ray and IR fluxes ensures that the selected sources will be above ROSAT and *WISE* sensitivity thresholds.

We apply our selection to the BL Lac objects that belong to the ROMA-BZCAT (Massaro et al. 2009; Massaro et al. 2010; Massaro et al. 2011b).

For the blazars listed in the ROMA-BZCAT we found 41 TBCs that meet our criteria. All these TBCs are detected by *Fermi* in the 30 MeV - 300 GeV energy range with only five exceptions: BZB J0056-0936, BZB J0214+5144, BZB J0809+3455, BZB J1215+0732 and BZB J1445-0326, in particular, about $\sim 90\%$ of them show hard γ -ray spectra (i.e., γ -ray photon index $\Gamma < 2$). Their complete list can be found in Table 3, where we report their ROMA-BZCAT name, that of their *WISE* counterpart, the redshift if known, the ROSAT X-ray flux corrected for the Galactic absorption (Kalberla et al. 2005), the *Fermi* γ -ray spectral index, the IR *WISE* colors together with the IR flux in the $3.4-12\mu\text{m}$ band and the value of Φ_{XIR} .

Finally, we note that, all the TBCs selected from the ROMA-BZCAT lie within 3σ level of confidence of the regression line (see Section 2.3), with the only exceptions of BZB J0214+5144 and BZB J1445-0326.

4. COMPARISON WITH PREVIOUS SELECTIONS

Several attempts to select BL Lac candidates for TeV observations have been carried out in the last decade, with particular attention to HBLs as in our analysis. Selection of source candidates has typically relied on the availability of source catalogs at lower frequencies that could reveal properties characteristic of VHE emitters. For instance, blazar candidates for VHE observations were typically selected from catalogs of hard X-ray sources (e.g., Stecker et al. 1996; Donato et al. 2001) or objects that had a particular combination of radio, optical and X-ray energy densities (Costamante & Ghisellini 2002).

In particular, Costamante & Ghisellini (2002) proposed a selection of BL Lac candidates for TeV observa-

TABLE 2
 THE COMPLETE LIST OF TeV DETECTED BL LAC OBJECTS (00 – 24 HH).

ROMA-BZCAT name	TeVCat name	WISE name	z	F_X cgs	F_{TeV} Crab	<i>Fermi</i> detect.	[3.4]-[4.6] mag	[4.6]-[12] mag	F_{IR} cgs	Φ_{XIR}
J0013-1854	SHBL J001355.9-185406	J001356.04-185406.5	0.094	6.49	0.01	no	0.22(0.03)	1.32(0.10)	1.36(0.08)	4.76
J0033-1921	KUV 00311-1938	J003334.36-192132.9	0.61?	8.43	—	yes	0.79(0.03)	2.14(0.04)	3.06(0.08)	2.75
J0035+5950	1ES 0033+595	J003552.62+595004.3	?	5.41	—	yes	0.66(0.03)	2.09(0.03)	2.46(0.06)	2.20
J0152+0147	RGB J0152+017	J015239.60+014717.4	0.08	3.13	0.02	yes	0.38(0.03)	1.71(0.04)	2.71(0.08)	1.16
J0222+4302	3C 66A	J022239.60+430207.8	0.444?	2.29	0.022	yes	0.84(0.03)	2.25(0.03)	36.87(0.70)	0.06
J0232+2017	1ES 0229+200	J023248.60+201717.3	0.139	5.63	0.018	no	0.30(0.04)	1.60(0.09)	1.19(0.07)	4.71
J0303-2407	PKS 0301-243	J030326.49-240711.4	0.26?	5.78	—	yes	0.86(0.03)	2.28(0.03)	8.50(0.17)	0.68
J0319+1845	RBS 0413	J031951.80+184534.6	0.19	8.33	0.01	yes	0.68(0.04)	2.06(0.09)	0.95(0.06)	8.79
J0349-1159	1ES 0347-121	J034923.18-115927.2	0.188	14.28	0.02	no	0.51(0.05)	1.57(0.27)	0.33(0.06)	43.57
J0416+0105	1ES 0414+009	J041652.48+010523.9	0.287	22.6	0.006	yes	0.68(0.04)	1.85(0.07)	1.63(0.07)	13.86
J0449-4350	PKS 0447-439	J044924.69-435008.9	0.205?	8.12	0.045	yes	0.84(0.03)	2.27(0.02)	16.43(0.31)	0.49
J0507+6737	1ES 0502+675	J050756.16+673724.3	0.416?	12.9	0.06	yes	0.71(0.03)	1.95(0.05)	1.89(0.06)	6.82
J0550-3216	PKS 0548-322	J055040.57-321616.4	0.069	26.3	0.013	no	0.23(0.03)	1.63(0.05)	1.99(0.06)	13.24
J0648+1516	RX J0648.7+1516	J064847.64+151624.8	0.179	10.3	0.033	yes	0.60(0.03)	1.89(0.06)	1.67(0.07)	6.18
J0650+2503	1ES 0647+250	J065046.48+250259.6	0.203?	13.0	0.03	yes	0.73(0.03)	2.10(0.04)	2.76(0.09)	4.70
J0710+5908	RGB J0710+591	J071030.05+590820.5	0.125	13.4	0.03	yes	0.49(0.03)	1.78(0.06)	1.52(0.06)	8.82
J0721+7120	S5 0716+714	J072153.44+712036.3	?	2.27	—	yes	0.98(0.03)	2.66(0.02)	69.98(1.29)	0.03
J0809+5218	1ES 0806+524	J080949.19+521858.3	0.138	8.26	0.018	yes	0.69(0.03)	2.07(0.03)	4.02(0.10)	2.06
J1010-3119	1RXS J101015.9-311909	J101015.98-311908.3	0.143	10.2	0.008	yes	0.47(0.03)	1.73(0.07)	1.31(0.06)	7.81
J1015+4926	1ES 1011+496	J101504.13+492600.8	0.212	13.2	0.07	yes	0.80(0.03)	2.21(0.03)	6.49(0.14)	2.03
J1103-2329	1ES 1101-232	J110337.62-232931.0	0.186	20.9	0.02	yes	0.54(0.03)	1.81(0.08)	1.18(0.06)	17.68
J1104+3812	Markarian 421	J110427.32+381231.9	0.03	180.0	0.3	yes	0.61(0.03)	1.99(0.02)	27.08(0.50)	6.65
J1136+7009	Markarian 180	J113626.42+700927.1	0.045	35.1	0.11	yes	0.41(0.03)	1.96(0.03)	5.87(0.12)	5.98
J1217+3007	1ES 1215+303	J121752.08+300700.7	0.13?	24.9	0.035	yes	0.83(0.03)	2.32(0.03)	9.62(0.19)	2.59
J1221+3010	1ES 1218+304	J122121.95+301037.2	0.182	16.3	0.08	yes	0.68(0.03)	2.06(0.04)	2.55(0.07)	0.10
J1221+2813	W Comae	J122131.69+281358.5	0.102	1.3	0.09	yes	0.85(0.03)	2.33(0.03)	13.5(0.27)	6.40
J1315-4236	1ES 1312-423	J131503.39-423649.7	0.105	8.85	0.004	no	0.28(0.04)	1.23(0.16)	0.66(0.06)	13.48
J1427+2348	PKS 1424+240	J142700.40+234800.1	?	3.57	0.05	yes	0.83(0.03)	2.25(0.02)	21.43(0.40)	0.17
J1428+4240	H 1426+428	J142832.62+424021.0	0.129	35.5	0.19	yes	0.50(0.03)	1.79(0.05)	1.46(0.05)	24.33
J1442+1200	1ES 1440+122	J144248.24+120040.3	0.163	7.82	0.01	yes	0.48(0.03)	1.70(0.06)	1.20(0.05)	6.50
J1517-2422	AP Lib	J151741.82-242219.4	0.048	1.05	0.02	yes	0.88(0.03)	2.61(0.03)	27.94(0.53)	0.04
J1555+1111	PG 1553+113	J155543.05+111124.4	?	17.9	0.034	yes	0.81(0.03)	2.15(0.03)	12.86(0.26)	1.39
J1653+3945	Markarian 501	J165352.22+394536.5	0.033	36.9	—	yes	0.46(0.03)	2.01(0.03)	19.5(0.37)	1.89
J1743+1935	1ES 1741+196	J174357.84+193509.3	0.084	4.23	0.008	yes	0.43(0.03)	1.89(0.04)	3.70(0.09)	1.14
J1959+6508	1ES 1959+650	J195959.84+650854.7	0.047	32.3	0.64	yes	0.62(0.03)	2.16(0.03)	7.66(0.15)	4.22
J2001+4352	MAGIC J2001+435	J200112.87+435252.8	?	—	0.22	yes	0.77(0.03)	2.16(0.03)	7.56(0.16)	—
J2009-4849	PKS 2005-489	J200925.39-484953.5	0.071	33.3	0.03	yes	0.74(0.03)	2.22(0.03)	17.92(0.35)	1.86
J2158-3013	PKS 2155-304	J215852.05-301332.0	0.116	324.0	0.15	yes	0.79(0.03)	2.13(0.03)	33.93(0.65)	9.55
J2202+4216	BL Lacertae	J220243.29+421640.0	0.069	1.58	0.03	yes	1.01(0.03)	2.60(0.03)	126.47(2.41)	0.01
J2250+3824	B3 2247+381	J225005.75+382437.3	0.119	2.45	0.002	yes	0.61(0.03)	1.89(0.04)	2.73(0.08)	0.90
J2347+5142	1ES 2344+514	J234704.83+514217.9	0.044	7.71	0.11	yes	0.29(0.03)	1.72(0.03)	5.52(0.13)	1.40
J2359-3037	H 2356-309	J235907.88-303740.5	0.165	40.2	0.02	yes	0.69(0.03)	2.05(0.06)	1.40(0.05)	28.67

Col. (1) ROMA-BZCAT name.
 Col. (2) TeVCat name.
 Col. (3) WISE name.
 Col. (4) ROMA-BZCAT redshift: ? = unknown, number? = uncertain.
 Col. (5) ROSAT X-ray flux in the 0.1-2.4 keV energy range in units of 10^{-12} erg cm $^{-2}$ s $^{-1}$.
 Col. (6) archival TeV flux as reported on the TeVCat.
 Col. (7) *Fermi* detection as reported in the 2FGL.
 Cols. (8,9) IR colors from WISE. Values in parentheses are 1σ uncertainties.
 Col. (10) WISE IR flux in the 3.4-12 μ m energy range in units of 10^{-12} erg cm $^{-2}$ s $^{-1}$.
 Col. (11) Φ_{XIR} defined according to § 2.

tions, not only restricted to the HBLs as in the present analysis. Their selection was mainly based on a fitting procedure of the broadband SEDs of a sample of BL Lacs compiled from literature with a homogeneous synchrotron self Compton model and calculating the expected TeV flux. They conclude that TeV BL Lac candidates are primarily selected to be bright both in X-rays and radio bands, as generally occurs for HBLs. Tavecchio et al. (2010) also proposed a selection of BL Lac candidates for TeV observations on the basis of the γ -ray properties, such as hard γ -ray spectra, of the *Fermi* sources detected in its first three months of operation. Recently, Massaro et al. (2011c) also outlined a criterion to select only TBCs, mainly based on the X-ray spectral curvature and applied to the HBLs detected in the major X-ray surveys as Einstein Slew Survey (e.g., Elvis et al.1992). This was the first criterion developed on the basis of the BL Lac spectral shape observed in a restricted energy range.

In comparison with the analyses cited above, 8 out of 41 of the TBCs selected were also present in their lists. We note that 2 sources appear in Stecker et al.

(1996) list of candidates and 8 in that of Costamante & Ghisellini (2002), with 2 objects, BZB J0326+0225 and BZB J1728+5013, present in both selections. Three of our sources appear as TeV candidates in the Tavecchio et al. (2010) selection: BZB J0109+1816, BZB J0136+3905 and BZB J1058+5628; the last source also in Costamante & Ghisellini (2002).

In Massaro et al. (2011c) we also propose a X-ray based selection and BZB J0326+0225, BZB J1136+6737, BZB J1417+2543, and BZB J1728+5013, were deeply investigated and selected as TBCs on the basis of their X-ray spectral curvature. In particular, BZB J1728+5013 is present in all the previous selections with the only exception of Tavecchio et al. (2010), making it the most promising TBC.

The main difference between our method and the previous selections is that it is based on the IR rather than on the radio flux density and that was built on the basis of the peculiar IR colors of the known TBLs (i.e., a surrogate of the IR spectral shape), an information that was not used in all the previous selections. It is also worth noting that all $\sim 90\%$ BL Lacs of the ROMA-BZCAT

TABLE 3
THE COMPLETE LIST OF TBCS SELECTED FROM THE ROMA-BZCAT (00 – 24 HH).

ROMA-BZCAT name	WISE name	z	F _X cgs	Γ	[3.4]-[4.6] mag	[4.6]-[12] mag	F _{IR} cgs	Φ _{XIR}	Sel.
BZB J0035+1515	J003514.71+151504.2	?	3.02	1.62	0.78(0.03)	2.20(0.06)	1.63(0.07)	1.86	—
BZB J0056-0936	J005620.06-093630.6	0.103	4.20	—	0.29(0.03)	1.75(0.05)	2.52(0.08)	1.67	—
BZB J0109+1816	J010908.17+181607.7	0.145	4.51	1.99	0.81(0.03)	2.28(0.05)	1.87(0.06)	2.42	T
BZB J0136+3905*	J013632.59+390559.2	?	9.60	1.69	0.79(0.03)	2.11(0.03)	4.01(0.09)	2.39	C,T
BZB J0209-5229	J020921.60-522922.7	?	7.98	1.91	0.61(0.03)	1.97(0.05)	1.58(0.05)	5.06	—
BZB J0214+5144	J021417.94+514451.9	0.049	4.58	—	0.29(0.03)	1.77(0.04)	3.48(0.09)	1.31	M
BZB J0238-3116	J023832.47-311657.9	?	5.14	1.85	0.64(0.03)	1.91(0.04)	1.96(0.06)	2.62	—
BZB J0316-2607	J031614.93-260757.2	0.443	3.05	1.87	0.75(0.03)	2.14(0.04)	1.34(0.04)	2.27	—
BZB J0325-1646	J032541.09-164616.8	0.291	27.2	1.97	0.70(0.04)	2.02(0.07)	1.10(0.05)	24.77	—
BZB J0326+0225	J032613.94+022514.7	0.147	12.0	2.06	0.58(0.04)	2.02(0.08)	1.19(0.06)	10.07	C,M,S
BZB J0505+0415	J050534.76+041554.5	0.027?	3.07	2.15	0.60(0.04)	2.03(0.08)	1.02(0.06)	3.02	—
BZB J0536-3343	J053629.06-334302.5	?	4.84	2.39	0.68(0.03)	2.04(0.05)	1.31(0.05)	3.70	—
BZB J0543-5532	J054357.21-553207.5	?	9.04	1.74	0.69(0.03)	2.00(0.04)	1.57(0.04)	5.75	—
BZB J0805+7534	J080526.63+753424.9	0.121	3.66	1.68	0.54(0.03)	2.02(0.04)	1.94(0.06)	1.89	—
BZB J0809+3455	J080938.91+345537.3	0.083	4.07	—	0.33(0.03)	1.69(0.07)	1.69(0.07)	2.40	—
BZB J0913-2103	J091300.22-210321.0	0.198	12.4	1.94	0.62(0.03)	2.06(0.04)	2.57(0.07)	4.83	—
BZB J0915+2933	J091552.40+293324.0	?	6.25	1.87	0.76(0.03)	2.24(0.04)	3.31(0.09)	1.89	—
BZB J1023-4336	J102356.20-433601.5	?	13.4	1.82	0.78(0.03)	2.06(0.04)	2.16(0.06)	6.19	—
BZB J1058+5628*	J105837.73+562811.3	0.143	3.13	1.93	0.80(0.03)	2.28(0.03)	6.07(0.13)	0.52	T
BZB J1117+2014	J111706.26+201407.5	0.138	33.6	1.70	0.61(0.03)	2.05(0.05)	1.98(0.07)	16.99	C
BZB J1120+4212	J112048.06+421212.6	0.124?	7.81	1.61	0.70(0.03)	1.98(0.07)	1.18(0.05)	6.62	—
BZB J1136+6737	J113630.10+673704.4	0.136	14.8	1.68	0.44(0.03)	1.87(0.06)	1.16(0.05)	12.71	C
BZB J1215+0732	J121510.98+073204.7	0.136	3.27	—	0.42(0.04)	1.76(0.08)	1.19(0.06)	2.75	—
BZB J1241-1455	J124149.40-145558.4	?	8.37	1.98	0.68(0.03)	2.04(0.06)	1.51(0.06)	5.55	—
BZB J1243+3627*	J124312.74+362744.0	?	10.0	1.70	0.78(0.03)	2.20(0.03)	3.97(0.09)	2.52	—
BZB J1248+5820	J124818.79+582028.8	?	3.99	1.95	0.86(0.03)	2.29(0.03)	7.59(0.15)	0.53	—
BZB J1417+2543	J141756.67+254325.9	0.237	15.3	1.98	0.53(0.03)	2.02(0.05)	1.16(0.04)	13.20	C,M
BZB J1439+3932	J143917.48+393242.8	0.344	11.1	1.69	0.72(0.03)	2.10(0.04)	1.99(0.05)	5.57	—
BZB J1443-3908	J144357.20-390839.9	0.065?	6.56	1.77	0.73(0.03)	2.16(0.03)	4.48(0.11)	1.46	—
BZB J1445-0326	J144506.24-032612.5	?	3.21	—	0.69(0.03)	1.86(0.08)	0.92(0.05)	3.48	—
BZB J1448+3608	J144800.59+360831.2	?	4.62	1.89	0.77(0.03)	2.13(0.04)	1.55(0.04)	2.99	—
BZB J1501+2238	J150101.83+223806.3	0.235	4.02	1.77	0.83(0.03)	2.28(0.03)	6.15(0.12)	0.65	—
BZB J1540+8155	J154015.90+815505.6	?	5.77	1.48	0.69(0.03)	2.00(0.04)	1.40(0.04)	4.12	C
BZB J1548-2251	J154849.76-225102.5	?	6.21	1.93	0.70(0.03)	2.11(0.05)	2.16(0.08)	2.88	—
BZB J1725+1152	J172504.34+115215.5	?	11.5	1.93	0.81(0.03)	2.16(0.03)	4.53(0.11)	2.54	C
BZB J1728+5013	J172818.63+501310.5	0.055	20.4	1.83	0.62(0.03)	2.18(0.03)	3.13(0.07)	6.52	C,M,S
BZB J1917-1921	J191744.82-192131.5	0.137	2.86	1.91	0.84(0.03)	2.27(0.03)	6.16(0.15)	0.46	—
BZB J2221-5225	J222129.30-522527.6	?	5.43	2.06	0.72(0.03)	2.17(0.05)	1.42(0.04)	3.83	—
BZB J2323+4210	J232352.07+421058.6	0.059?	2.69	1.88	0.77(0.03)	2.28(0.07)	1.09(0.05)	2.47	—
BZB J2324-4040	J232444.65-404049.3	?	14.6	1.81	0.75(0.03)	2.06(0.03)	4.77(0.11)	3.06	—
BZB J2340+8015	J234054.23+801515.9	0.274	3.39	1.87	0.75(0.03)	2.12(0.04)	2.48(0.06)	1.37	—

Col. (1) ROMA-BZCAT name. Asterisk indicates sources observed by VERITAS and not detected at TeV energies (Aliu et al. 2012, see also Section 6).

Col. (2) WISE name.

Col. (3) ROMA-BZCAT redshift: ? = unknown, number? = uncertain.

Col. (4) ROSAT X-ray flux in the 0.1-2.4 keV energy range in units of 10^{-12} erg cm $^{-2}$ s $^{-1}$, corrected for the Galactic absorption (Kalberla et al. 2005).

Col. (5) 2FGL γ -ray photon index Γ .

Cols. (6,7) IR colors from WISE. Values in parentheses are 1σ uncertainties.

Col. (8) WISE IR flux in the 3.4-12 μ m energy range in units of 10^{-12} erg cm $^{-2}$ s $^{-1}$.

Col. (9) Φ_{XIR} defined according to § 2. Col. (10) We indicate if the source was also selected by different, previous, analyses performed by Stecker et al. (1996; - S), Costamante & Ghisellini (2002; - C), Tavecchio et al. (2010; - T), and Massaro et al. (2012c; - M) (see § 4 for more details).

that met our criteria are also detected in the γ -rays by *Fermi*, while this was not a requirement for our selection.

5. ALL-SKY INFRARED SEARCH OF TBL CANDIDATES

We extended our search of TBCs beyond the ROMA-BZCAT catalog by considering X-ray sources from the ROSAT bright source catalog (Voges et al. 1999) with a counterpart in the WISE all-sky survey (Wright et al. 2010) and adopting less restrictive criteria than the one previously described in § 3.

We considered all the IR sources detected by WISE that lie within the positional uncertainty of an X-ray source in the ROSAT bright source catalog. Then, we selected only IR sources with WISE magnitudes smaller than 13.32 mag, 12.64 mag and 10.76 mag at 3.4 μ m, 4.6 μ m and 12 μ m, respectively, IR colors between 0.23 mag < [3.4]-[4.6] < 0.86 mag 1.60 mag < [4.6]-[12] < 2.32 mag and δ < 1 (see § 2.3 and § 3 for more details). This criterion corresponds to a less restrictive selection than the one previously proposed, because it is not based on the X-ray flux nor on the ratio Φ_{XIR} .

The ROSAT bright source catalog lists 18811 X-ray sources all-sky, however only 189 of them met the criteria outlined above. All of them are unique associations be-

tween the ROSAT and the WISE all-sky surveys. Moreover, out of the 189 selected sources, 93 are associated to sources listed in the ROMA-BZCAT catalog. These were excluded from our extended TBL candidate list to avoid redundancy in the selections.

For the remaining 96 sources, we performed a multifrequency analysis to select the most reliable TBCs. We searched in the following major radio, IR, optical databases as well as in the NASA Extragalactic Database (NED)⁹ for any possible counterpart within 3".3 to verify if additional information can confirm their BL Lac nature.

For the radio surveys we searched in the catalogs of the NRAO VLA Sky Survey (NVSS; Condon et al. 1998), the VLA Faint Images of the Radio Sky at Twenty-Centimeters (FIRST; Becker et al. 1995; White et al. 1997), the Sydney University Molonglo Sky Survey (SUMSS; Mauch et al. 2003) and the The Australia Telescope 20 GHz Survey (AT20G; Murphy et al. 2010) surveys; for the IR we compare our list only with the Two Micron All Sky

⁹ <http://ned.ipac.caltech.edu/>

Survey (2MASS; Skrutskie et al. 2006) since each *WISE* source is already associated with the closest 2MASS source by default in the *WISE* catalog (see Cutri et al. 2012, for more details). Then, we also searched for optical counterparts, with possible spectra available, in the Sloan Digital Sky Survey (SDSS; e.g. Adelman et al. 2008; Paris et al. 2012) and in the Six-degree-Field Galaxy Redshift Survey (6dFGS; Jones et al. 2004; Jones et al. 2009); in the hard X-rays within the 2nd Palermo BAT catalog (2PBC; Cusumano et al. 2010) and if associated with *Fermi* source in the 2FGL (Nolan et al. 2012). We also searched the USNO-B Catalog (Monet et al. 2003) for the optical counterparts within 3".3 and we report the magnitude in the R band in Table 4. Our final list has been also compared with the recent *WISE*-2MASS-ROSAT selection of active galaxies proposed by Edelson & Malkan (2012).

On the basis of our multifrequency investigation we selected 54 TBCs out of the 96 remaining sources selected combining the ROSAT all-sky survey with the *WISE* observations. All these new 54 TBCs are listed in Table 4 together with the results of our multifrequency analysis and their salient parameters as the IR *WISE* colors and, if present, the 2FGL association (e.g., Ackermann et al. 2011; Nolan et al. 2012).

A large fraction of our TBCs (~55%) have a clear radio counterpart in one of the major radio surveys as occurs for all the BL Lacs that belong to the *WISE* Gamma-ray strip. In particular, 21 out of 54 sources have a radio counterpart in the NVSS, 4 in the SUMSS, one in both radio surveys while only 2 objects have a correspondence in the FIRST. All our 54 TBCs are detected in the 2MASS catalog and they are also detected by *WISE* at 22 μ m with two exceptions. Optical spectra are available in literature for 5 TBCs listed in Table 4 all classified as BL Lac objects, thus no optical spectroscopic observations are necessary to confirm their nature. Then, 21 out of 54 TBCs have been observed by the 6dFGS and 4 by the SDSS. At high energies only one source has been detected by *Swift*-BAT hard X-ray survey while 14 out of 54 objects have been associated or lie within the positional uncertainty region of a *Fermi* source listed in the 2FGL. It is worth noting that 14 out of 54 TBCs are associated with *Fermi* sources as listed in the 2FGL catalog and in the 2LAC catalogs, being classified as AGNs of uncertain type (Nolan et al. 2012; Ackermann et al. 2011). In particular, 1RXS J083158.1-180828, 1RXS J130421.2-435308 and 1RXS J204745.9-024609 are the only three sources that belong to our final list of TBCs selected combining *WISE* and ROSAT all-sky catalogs that were also selected as active galaxies of uncertain nature by Edelson & Malkan (2012).

Moreover, 16 X-ray sources out of 54 TBCs were previously unidentified in the ROSAT all-sky catalog (Voges et al. 1999) (i.e., without a counterpart assigned at lower energies). The existence of an IR *WISE* counterpart in the *WISE* catalog, with similar colors than those of γ -ray BL Lacs suggests that these could be potential BL Lac candidates. We note that none of these 54 TBCs is listed in the Sedentary Survey of extreme HBLs (Giommi et al. 2005), thus highlighting that our method is successful to select BL Lacs without including

any criteria based on the radio observations.

Forty-two out of 189 IR-X-ray sources we selected have multiwavelength archival observations that indicate they are not BL Lacs. This suggests that a contamination of ~22% of non-BL Lac objects could be present in our selected sample. We will be able to make a more accurate estimate of the contamination once all the optical spectroscopic information will be available for our sample.

Finally, we note that all the TBCs selected from the ROSAT bright source catalog with a counterpart in the *WISE* all-sky survey lie within 3 σ level of confidence of the regression line (see Section 2.3), with the only exceptions of 5 sources, namely: 1RXS J072812.1+671821, 1RXS J132908.3+295018, 1RXS J180219.5-245157, 1RXS J183821.0-602519 and 1RXS J193320.3+072616.

6. SUMMARY AND CONCLUSIONS

Previous studies based on the *WISE* all-sky survey have revealed that the IR spectral shape of high frequency peaked BL Lacs detected at TeV energies (TBLs) can be successfully used to associate γ -ray BL Lacs (e.g., Massaro et al. 2011a; Massaro et al. 2012b; D'Abrusco et al. 2013). In this paper, we extended the same technique to search for high frequency peaked BL Lacs that could be candidates for future TeV observations (i.e., TBCs), by selecting sources with similar IR and X-ray properties of the known TBLs.

Known TBLs populate a subregion of the *WISE* Gamma-ray Strip (Massaro et al. 2012a; D'Abrusco et al. 2013), defined in the [3.4]-[4.6]-[12] μ m IR color-color space. Then, on the basis of their IR and the X-ray emission, we identify 41 TBCs among the BL Lacs listed in the ROMA-BZCAT catalog (Massaro et al. 2009; Massaro et al. 2011b).

A comparison between our list of TBCs, chosen out of the ROMA-BZCAT catalog, with previous selections (Stecker et al. 1996; Costamante & Ghisellini 2002; Tavecchio et al. 2010; Massaro et al. 2011c) finds good agreement (see § 4). Our new criteria, mainly based on the IR colors, a surrogate of the spectral shape of the low energy component for the BL Lac objects, is not based on radio or γ -ray data. Moreover, our IR selection was built only in the 2-dimensional [3.4]-[4.6]-[12] μ m color-color diagram, while all our previous selections of γ -ray blazar candidates, mostly developed to associate unidentified gamma-ray sources (Massaro et al. 2012b; D'Abrusco et al. 2013), required the IR detection in all four *WISE* bands. All the BL Lacs of the ROMA-BZCAT that met our criteria are also detected in the γ -ray band by *Fermi*, while this was not a requirement for the selection discussed in this paper.

We note that VERITAS observations have been performed for 3 of our TBCs selected within the ROMA-BZCAT: BZB J0136+3905, BZB J1058+5628 and BZB J1243+3627 (Aliu et al. 2012). However, as discussed in Aliu et al. (2012), both BZB J0136+3905 and BZB J1243+3627 do not have a redshift estimate, indicating that their non TeV-detection could be due the absorption of high energy photons by the extragalactic background light (Franceschini et al. 2008). On the other hand, BZB J1058+5628 was found variable in the γ -rays by *Fermi* during the same period of the VERITAS observations.

Thus, the non-detection at TeV energies of these three sources does not affect our selection that can only be verified with additional TeV observations.

We conducted an extended search based on less restrictive criteria based on the combination of the *WISE* and ROSAT observations to search for new TBCs with IR properties similar to those of the TBLs in the X-ray sky. We found additional 54 sources that could be considered TBCs with pending confirmation of their BL Lac nature with follow-up optical spectroscopy. We also note that 16 TBCs out of 54 X ray sources were previously unidentified in the ROSAT bright source catalog (Voges et al. 1999); then we provide the first association with a low energy counterpart correspondent to our TBCs selected on the basis of the IR *WISE* colors. We note that only 21 out of a total of 95 TBCs (i.e., 41 selected in the ROMA-BZCAT and 54 in the all-sky search) have a reliable redshift determination. The TBC with the highest redshift is BZB J0316-2607 at $z=0.443$ closer than the most distant TeV source: 3C 279 at $z=0.5362$ (e.g., Errando et al. 2008).

Our investigation provides new targets to plan observations with ground based Cherenkov telescopes such as HESS, MAGIC and VERITAS or in the near future with CTA.

We thank the anonymous referee for useful comments that improved the presentation of our work. We are grateful to R. Mukherjee for her valuable comments and suggestions that improved the manuscript as well as to S. Digel, P. Giommi, D. Harris and J. Grindlay for their helpful discussions. The work is supported by the NASA grants NNX12AO97G. R. D’Abrusco grate-

fully acknowledges the financial support of the US Virtual Astronomical Observatory, which is sponsored by the National Science Foundation and the National Aeronautics and Space Administration. The work by G. Tosti is supported by the ASI/INAF contract I/005/12/0. M. Errando acknowledges support from the NASA grant NNX12AJ30G. TOPCAT¹⁰ (Taylor 2005) was used extensively in this work for the preparation and manipulation of the tabular data and the images. Part of this work is based on archival data, software or on-line services provided by the ASI Science Data Center. This research has made use of data obtained from the High Energy Astrophysics Science Archive Research Center (HEASARC) provided by NASA’s Goddard Space Flight Center; the SIMBAD database operated at CDS, Strasbourg, France; the NASA/IPAC Extragalactic Database (NED) operated by the Jet Propulsion Laboratory, California Institute of Technology, under contract with the National Aeronautics and Space Administration. Part of this work is based on the NVSS (NRAO VLA Sky Survey); The National Radio Astronomy Observatory is operated by Associated Universities, Inc., under contract with the National Science Foundation. This publication makes use of data products from the Two Micron All Sky Survey, which is a joint project of the University of Massachusetts and the Infrared Processing and Analysis Center/California Institute of Technology, funded by the National Aeronautics and Space Administration and the National Science Foundation. This publication makes use of data products from the Wide-field Infrared Survey Explorer, which is a joint project of the University of California, Los Angeles, and the Jet Propulsion Laboratory/California Institute of Technology, funded by the National Aeronautics and Space Administration.

REFERENCES

- Abdo, A. A., et al. 2009, *Astroparticle Physics*, 32, 193
 Abdo, A. A. et al. 2010 *ApJS* 188 405
 Ackermann, M. et al. 2011 *ApJ*, 743, 171
 Ackermann, M. et al. 2012 *ApJ*, 753, 83
 Adelman-McCarthy, J., Agueros, M.A., Allam, S.S., et al. 2008, *ApJS*, 175, 297
 Ali, E. et al. 2012 *ApJ*, 759, 102
 Becker, R. H., White, R. L., Helfand, D. J. 1995 *ApJ*, 450, 559
 Blandford, R. D., Rees, M. J., 1978b *PhyS*, 17, 265
 Blandford, R. D. & Königl, A. 1979 *ApJ*, 232, 34
 Condon, J. J., Cotton, W. D., Greisen, E. W., Yin, Q. F., Perley, R. A., Taylor, G. B., & Broderick, J. J. 1998, *AJ*, 115, 1693
 Costamante, L. & Ghisellini, G. 2002 *A&A*, 384, 56
 Cusumano, G. et al. 2010 *A&A*, 524A, 64
 Cutri et al. 2012 wise.rept, 1C
 D’Abrusco, R., Massaro, F., Ajello, M., Grindlay, J. E., Smith, Howard A. & Tosti, G. 2012 *ApJ*, 748, 68
 D’Abrusco, R., Massaro, F., Paggi, A., Masetti, N., Giroletti, M., Tosti, G. et al. 2013 *ApJS* submitted
 Donato, D., Ghisellini, G., Tagliaferri, G. & Fossati, G., 2001, *A&A*, 375, 739
 Edelson, R. & Malkan, M. 2012 *ApJ*, 751, 52
 Elvis, M., Plummer, D., Schachter, J., Fabbiano, G. 1992 *ApJS*, 80, 257
 Errando, M., Bock, R., Kranich, D., Lorenz, E., Majumdar, P., Mariotti, M., Mazin, D., Prandini, E. et al. 2008 *AIPC*, 1085, 423
 Franceschini, A., Rodighiero, G., Vaccari, M. 2008 *A&A*, 487, 837
 Giommi, P. et al. 2005, *A&A*, 434, 385
 Giommi, P. et al. 2007 *A&A*, 468, 571
 Giommi, P., Colafrancesco, S., Padovani, P., Gasparrini, D., Cavazzuti, E., Cutini, S. 2009, *A&A*, 508, 107
 Giommi, P. et al. 2012a *A&A*, 541A, 160
 Giommi, P., Padovani, P., Polenta, G., Turriziani, S., D’Elia, V., Piranomonte, S. 2012b *MNRAS*, 420, 2899
 González-Nuevo, J. et al. 2010 *A&A*, 518, L38
 Hartman, R.C. et al., 1999 *ApJS* 123
 Howard, W. E. III, Dennis, T. R., Maran, S. P.; Aller, H. D. 1965 *ApJS*, 10, 331
 Kalberla, P.M.W., Burton, W.B., Hartmann, D., 2005, *A&A*, 440, 775
 Impey, C. D. & Neugebauer, G. 1988 *AJ*, 95, 307
 Jones, H. D. et al. 2004 *MNRAS*, 355, 747
 Jones, H. D. et al. 2009 *MNRAS*, 399, 683
 Landau, R., Golish, B., Jones, T. J., et al. 1986, *ApJ*, 308, L78
 Laurent-Muehleisen, S. A., Kollgaard, R. I., Feigelson, E. D., Brinkmann, W., Siebert, J. 1999 *ApJ*, 525, 127
 Maselli, A., Massaro, E., Nesci, R., Sclavi, S., Rossi, C., Giommi, P. 2010a *A&A*, 512A, 74
 Maselli, A., Cusumano, G., Massaro, E., La Parola, V., Segreto, A., Sbarufatti, B. 2010b *A&A*, 520A, 47
 Massaro, E., Perri, M., Giommi, P., et al. 2004, *A&A*, 422, 103
 Massaro, F. et al. 2008a *A&A*, 489, 1047
 Massaro, F., Tramacere, A., Cavaliere, A., Perri, M., Giommi, P. 2008b *A&A*, 478, 395
 Massaro, E., Giommi, P., Leto, C., Marchegiani, P., Maselli, A., Perri, M., Piranomonte, S., Sclavi, S. 2009 *A&A*, 495, 691
 Massaro, E., Giommi, P., Leto, C., Marchegiani, P., Maselli, A., Perri, M., Piranomonte, S., Sclavi, S. 2010
<http://arxiv.org/abs/1006.0922>
 Massaro, F., D’Abrusco, R., Ajello, M., Grindlay, J. E. & Smith, H. A. 2011 *ApJ*, 740L, 48

¹⁰ <http://www.star.bris.ac.uk/~mbt/topcat/>

APPENDIX

To further justify the classification scheme proposed in Section 2.1 based on Φ_{XIR} , we assumed a broadband description of the BL Lac spectra, from the IR to the X-rays, in the form of a log-parabola (e.g., Howard et al. 1965; Landau et al. 1986), expressed as:

$$S_\nu = \frac{S_p}{\nu} \cdot \left(\frac{\nu}{\nu_p} \right)^{-b \log(\nu/\nu_p)} \text{ erg cm}^{-2} \text{ s}^{-1} \text{ Hz}^{-1} \quad (1)$$

where ν_p is the SED peak frequency, S_p the SED peak flux at ν_p , and b the spectral curvature (see Massaro et al. 2004; Tramacere et al. 2007, for more details). We computed the ratio Φ_{XIR} as function of the peak frequency ν_p for different values of b as shown in Figure 3. Thus for values of ν_p larger than 10^{15} Hz, as generally seen for HBLs, Φ_{XIR} is systematically larger than 0.1 (see Figure 3). Values of spectral curvature used in Figure 3 are those typically observed in BL Lac objects (Massaro et al. 2008a; Massaro et al. 2008b; Massaro et al. 2011b).

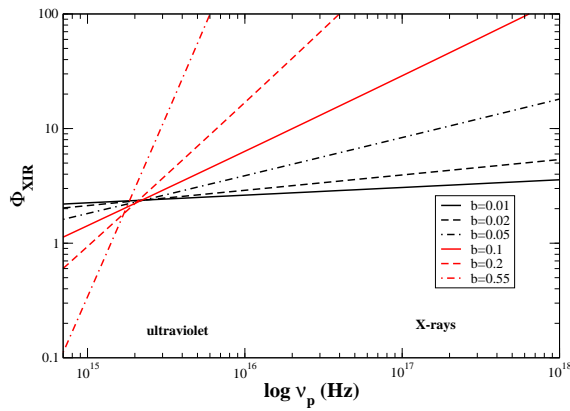


FIG. 3.— The values of Φ_{XIR} as function of the peak frequency ν_p of the log-parabolic function (see Eq. 1) assumed as simple representation of the low energy component of the BL Lac SED. The different lines correspond to different values of the spectral curvature b , typical of BL Lac objects (e.g., Massaro et al. 2008a; Massaro et al. 2008b).